

N,N-bis(Cyclohexanol)amine Aryl Esters: A New Class of Highly Potent Transporter-Dependent Multidrug Resistance Inhibitors

Cecilia Martelli,[†] Daniela Alderighi,[‡] Marcella Coronello,[§] Silvia Dei,[†] Maria Frosini,[‡] Bénédicte Le Bozec,^{||} Dina Manetti,[†] Annalisa Neri,[‡] Maria Novella Romanelli,[†] Milena Salerno,^{||} Serena Scapecchi,[†] Enrico Mini,[§] Giampietro Sgaragli,[‡] and Elisabetta Teodori^{*†}

Dipartimento di Scienze Farmaceutiche, Università di Firenze, via U. Schiff 6, 50019 Sesto Fiorentino (FI), Italy, Dipartimento di Neuroscienze, Sezione di Farmacologia, Fisiologia e Tossicologia, Università di Siena, via A. Moro 2, 53100 Siena, Italy, Dipartimento di Farmacologia Preclinica e Clinica, Università di Firenze, Viale Pieraccini 6, 50139 Firenze, Italy, Laboratoire de Biophysique Moléculaire, Cellulaire et Tissulaire (BioMoCeTi), UMR CNRS 7033, UMPC Université Paris 6 and Université Paris 13, 74 rue Marcel Cachin, 93017 Bobigny, France

Received October 8, 2008

A new series of Pgp-dependent MDR inhibitors having a *N,N*-bis(cyclohexanol)amine scaffold was designed on the basis of the frozen analogue approach. The scaffold chosen gives origin to different geometrical isomers. The new compounds showed a wide range of potencies and efficacies on doxorubicin-resistant erythroleukemia K562 cells in the pirarubicin uptake assay. The most interesting compounds (isomers of **3**) were studied further evaluating their action on the ATPase activity present in rat small intestine membrane vesicles and doxorubicin cytotoxicity potentiation on K562 cells. The latter assay was performed also on the isomers of **4**. The four isomers of each set present different behavior in each of these tests. Compound **3d** shows the most promising properties as it was able to completely reverse Pgp-dependent pirarubicin extrusion at low nanomolar concentration, inhibited ATPase activity at 5×10^{-9} and increased the cytotoxicity of doxorubicin with a reversal fold (RF) of 36.4 at $3 \mu\text{M}$ concentration.

Introduction

Multidrug resistance (MDR) is a kind of acquired drug resistance of cancer cells and microorganisms to a variety of chemotherapeutic drugs that usually are structurally and mechanistically unrelated.¹ Multidrug resistance may originate from several biochemical mechanisms; classical MDR² is due to a lower cell concentration of cytotoxic drugs associated with accelerated efflux of the chemotherapeutic agent as a consequence of the overexpression of proteins such as ABCB1 (Pgp) and ABCC1 (MRP1)³ that act as extrusion pumps. These proteins belong to the ABC superfamily of transporters that use ATP as energy source, but several families of similar pumps that use a variety of energy sources are present in mammals and microorganisms.^{1,4} In mammals, these proteins have been found in several important tissues besides cancer cells and blood–tissue barriers where they apparently regulate the secretion of physiologically important lipophilic molecules⁵ and the extrusion of xenobiotics that enter the organism.⁶

Direct information on the structure of Pgp and MRP1 is scarce,^{7,8} but resolution of the structure of homologous bacterial transporters^{9–11} has opened the way to the development of homology models^{12–14} and provided many useful details on the structure of the recognition site of ABC transporters. All information collected so far points to the existence of a large, polymorphous drug recognition domain, where a variety of molecules can be accommodated in a plurality of binding modes

through π – π , ion– π , hydrogen bond, and hydrophobic interactions.^{15–17}

Inhibition of the functions of Pgp, MRP1, and sister proteins is considered a suitable approach to circumvent MDR and drugs possessing inhibitory properties have been and are actively being sought,^{18–22} even if so far, no drug has been approved for therapy.^{23,24} An emerging potential use of these agents may be to increase drug penetration through biologically important protective barriers, such as the blood–brain and blood–cerebrospinal fluid barriers.²⁵ The main problems associated with the development of effective Pgp-mediated MDR inhibitors seem due to poor specificity, low potency, interference with physiological functions and, as a consequence, interference with the pharmacokinetics of the chemotherapeutic drug used.

Recently, we have described a new family of MDR reverters, endowed with fairly good potency, designed on the basis of a new concept arising from the emerging picture of the substrate recognition sites of Pgp, MRP1, and sister proteins.²⁶ In brief, we guessed that flexible molecules carrying a basic nitrogen flanked, at suitable distances, by two (or three) aromatic moieties, would accommodate in the recognition cavity choosing the most productive binding modes and therefore would interact with high affinity with the protein. The good potencies of most of the compounds synthesized and studied confirmed our prediction that the entropy toll paid had been compensated by the enthalpy gain due to the fact that flexible molecules can optimize their interaction within the recognition site.

Building on the results obtained and having in mind possible therapeutic applications, we have decided to verify the consequences of a partial reduction of the very high flexibility of our compounds. In fact, it has empirically been shown that a high number of rotatable bonds is detrimental for good absorption and drug-likeness,^{27,28} while it is well-known that flexibility does not favor selectivity. Toward this end, we designed a new series of molecules where the *N,N*-bis-arylalkylamine moiety of pre-

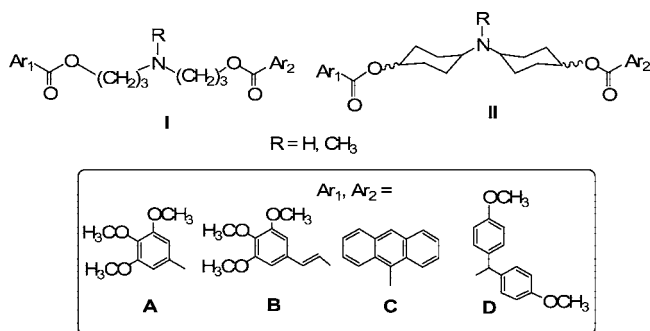
* To whom correspondence should be addressed. Phone: ++39 055 4573693. Fax: + 39 055 4573671. E-mail: elisabetta.teodori@unifi.it.

[†] Dipartimento di Scienze Farmaceutiche, Università di Firenze.

[‡] Dipartimento di Neuroscienze, Sezione di Farmacologia, Fisiologia e Tossicologia, Università di Siena.

[§] Dipartimento di Farmacologia Preclinica e Clinica, Università di Firenze.

^{||} Laboratoire de Biophysique Moléculaire, Cellulaire et Tissulaire (BioMoCeTi), UMR CNRS 7033, UMPC Université Paris 6 and Université Paris 13.

Chart 1. General Structures of Designed Compounds

vious series (general structure **I**) was substituted with that of *N,N*-bis-cyclohexylamine (general structure **II**) (Chart 1). The aromatic moieties selected were those that gave the best results in the linear series.

The scaffold chosen gives origin to four geometrical isomers (three when the two aryl groups are identical) of quite different shape that somehow represent restricted conformation analogues of the parent linear compounds. According to the frozen analogue approach,²⁹ they can provide further insight on the characteristics of the recognition site.

Preliminary results of this research have been published.³⁰ In the present paper, the set of studied compounds has been extended to evaluate SARs. The new compounds were synthesized and tested either as single isomers (compounds **3–8**) or as a 1:1 mixture of *cis/trans* (a) + *trans/trans* (b) isomers (compounds **9** and **10**). Mixtures **9a/b** and **10a/b** were not separated into the isomers because their MDR-reversing activity was less interesting than that of compounds **3–8**, a fact which suggested skipping the time-consuming preparation of the single isomers.

A variety of assays are available to test the modulating activity of MDR reverters, in particular those acting on Pgp.^{31–33} Pirarubicin erythroleukemia K562 cell uptake assay was used as a preliminary screening. The pharmacological profile of the compounds that showed the best results in this assay, was further studied evaluating their action on the ATPase activity present in rat small intestine membrane vesicles (**3a–d**) and doxorubicin cytotoxicity potentiation (RF) on doxorubicin-resistant erythroleukemia K562 cells (**3a–d** and **4a–d**).

Chemistry

The reaction pathways used to synthesize the desired compounds (**3–10**) are described in Scheme 1; their chemical and physical characteristics are reported in Table S1 (Supporting Information).

The 4-oxocyclohexyl esters **11–13** were obtained by esterification of 4-hydroxycyclohexanone³⁴ with 3,4,5-trimethoxybenzoyl chloride, *trans*-3-(3,4,5-trimethoxyphenyl)acryloyl chloride, or anthracene-9-carbonyl chloride, respectively. Reductive amination of compounds **11–13** with *trans*-4-aminocyclohexanol gave compounds **14a/b**, **15a/b**, and **16a/b**, while the same reaction of compounds **11** and **12** with *cis*-4-aminocyclohexanol³⁵ gave compounds **14c/d** and **15c/d**; in both cases, titanium(IV) isopropoxide as Lewis acid catalyst and NaBH₃CN as reducing agent were used, according to the Mattson procedure.³⁶ The secondary amines obtained were an approximately 1:1 mixture of *cis/trans* and *trans/trans* isomers (a/b) or *cis/cis* and *trans/cis* isomers (c/d), respectively, as results from ¹H NMR spectra.

A chromatographic separation was performed on the amines **14a/b**, **14c/d**, **15a/b**, and **15c/d** and the pure isomers **14a–d**

and **15a–d** were obtained. Their configuration was attributed on the basis of the ¹H NMR characteristics of the cyclohexane protons H1, H4 and H1', H4' as exemplified in Table S2 (Supporting Information) for compounds **14**, **17**, **3**, and **4**. In most cases, it was possible to extract the *J_{aa}* and sometimes the *J_{ae}* constants; when the signal does not allow extraction of the coupling constants, the half-height amplitude of the signal (*w/2*)^{37–39} allows confident attribution of the equatorial or axial nature of the protons. Moreover the chemical shift of the signal is diagnostic, because axial protons resonate at higher fields, while the corresponding equatorial ones are deshielded. For example, the isomers **14a** and **14c** present the H1 proton with equatorial characteristics ($\delta = 5.12$ ppm, *w/2* = 15.6 Hz and $\delta = 5.15$ ppm, *w/2* = 11.8 Hz, respectively), while isomers **14b** and **14d** present the H1 proton with axial characteristics ($\delta = 4.92$ ppm, *J_{aa}* = 10.8 Hz, *J_{ae}* = 4.4 Hz and $\delta = 4.93$ ppm, *J_{aa}* = 10.8 Hz, *J_{ae}* = 4.4 Hz, respectively). The isomers **14a** and **14b** present the H1' proton with axial characteristics ($\delta = 3.60$ ppm, *J_{aa}* = 10.6 Hz, *J_{ae}* = 4.0 Hz and $\delta = 3.62$ ppm, *J_{aa}* = 10.6 Hz, *J_{ae}* = 4.0 Hz, respectively) while isomers **14c** and **14d** present the H1' proton with equatorial characteristics ($\delta = 3.94$ ppm, *w/2* = 10.9 Hz for both isomers). Furthermore, the protons of the two carbon atoms carrying the amine function have axial characteristics in every isomer of **14** (see Table S2, Supporting Information), indicating that the two cyclohexane rings are in a *cis/trans* (**14a**), *trans/trans* (**14b**), *cis/cis* (**14c**), and *trans/cis* (**14d**) configuration. Therefore, ¹H NMR data show that **14a** and **14c** are frozen in a conformation having the bulky substituent in position 1 forced into an axial position, while **14b** and **14d** have the same group in the more relaxed equatorial position.

Reductive methylation of **14a–d**, **15a–d**, and **16a/b** with HCOOH/HCHO gave the corresponding tertiary amines **17a–d**, **18a–d**, and **19a/b**. The amino function of the secondary amine mixture **14a/b** was protected by transformation into the *t*-butylcarbamate (*t*-BOC^a) to give the mixture **20a/b**, which was then reacted with *trans*-3-(3,4,5-trimethoxyphenyl)acryloyl chloride to give **21a/b**, which, in turn, was transformed into **10a/b** by acidic cleavage with CF₃COOH. Final compounds **3a–d**, **4a–d**, **5a–d**, **6a–d**, **7a–c**, **8a–c**, and mixture **9a/b** were then obtained by reaction of **17a–d**, **18a–d**, and mixture **19a/b** with the proper acyl chloride.

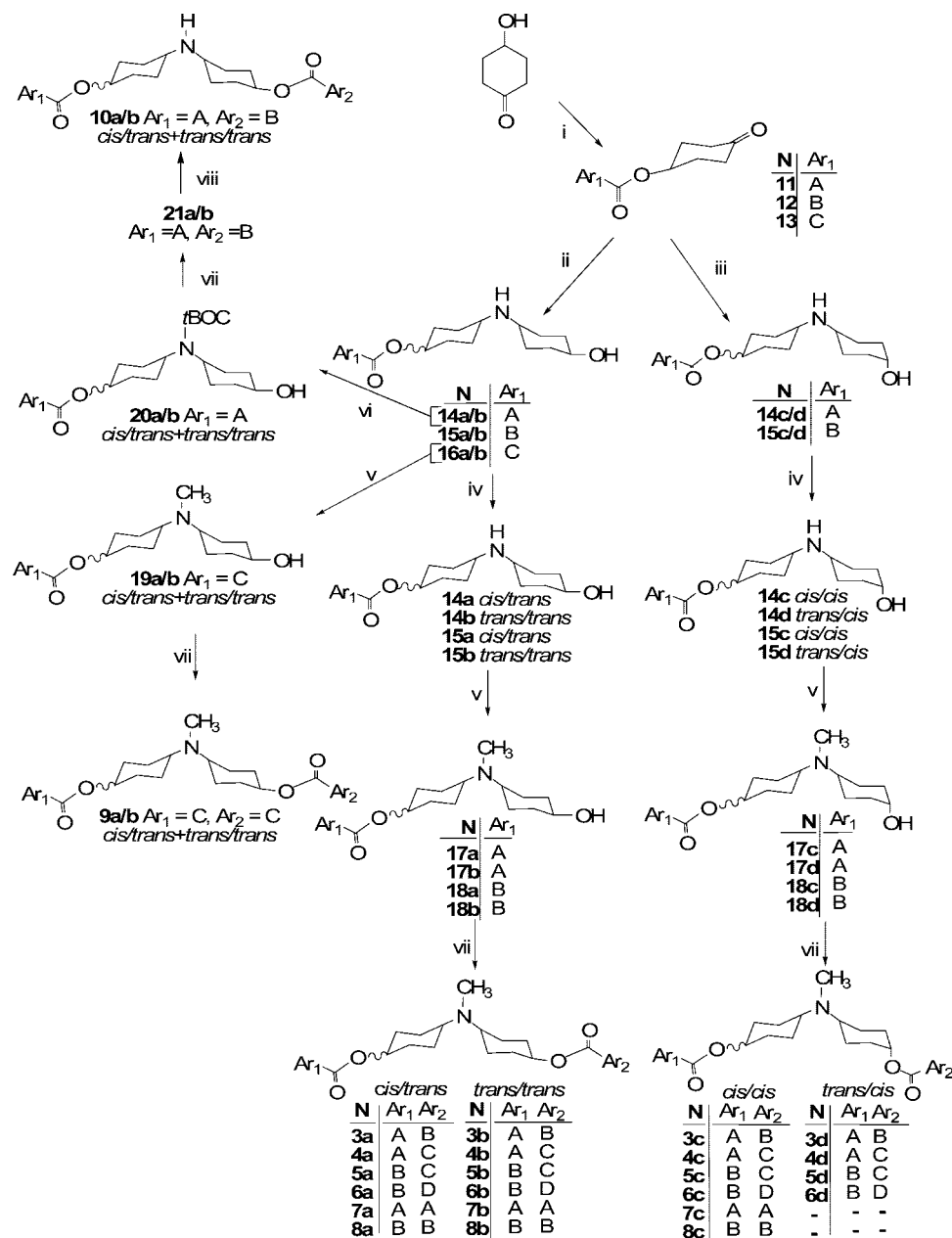
The ¹H NMR data, reported in Table S2 (Supporting Information), show that the configurations of **14a–d** are maintained in compounds **17a–d** and in the final products **3a–d**, **4a–d**, ruling out any isomerization in the subsequent reactions. The same behavior is detectable for the intermediates **15a–d**, **18a–d**, and final compounds **5a–d**, **6a–d**, **7a–c**, and **8a–c**.

The information on preferred conformations obtained from ¹H NMR was confirmed by molecular modeling (Figure 1) where isomers **3a–d** are shown in their lowest energy conformation with the 3,4,5-trimethoxybenzoate group in axial position. The lowest energy conformations of the set of isomers **4–8** are practically identical.

Pharmacological Studies

Modulation of Pirarubicin Uptake. The ability of compounds **3–10** to modulate Pgp action was evaluated on doxorubicin-resistant erythroleukemia K562 cells (K562/DOX) that, as reported in the literature, overexpress only Pgp.^{40,41} As

^a Abbreviations: RF, reversal fold; MTT, 3-(4,5-dimethylthiazolyl-2)-2,5-diphenyltetrazolium bromide; abs EtOH, absolute ethanol; (*i*-PrO)₄Ti, titanium (IV) isopropoxide; *t*-BOC, *t*-butylcarbamate.

Scheme 1. Synthesis of Compounds 3–10^a

^a Reagents and conditions: (i) $CHCl_3$, Ar_1COCl (3,4,5-trimethoxybenzoyl chloride, *trans*-3-(3,4,5-trimethoxyphenyl)acryloyl chloride, anthracene-9-carbonyl chloride); (ii) *trans*-4-aminocyclohexanol, $(i\text{-PrO})_4Ti$, $NaBH_3CN$; (iii) *cis*-4-aminocyclohexanol, $(i\text{-PrO})_4Ti$, $NaBH_3CN$; (iv) chromatographic separation; (v) $HCOOH/HCHO$; (vi) $(t\text{-BuOCO})_2O/Et_3N$; (vii) Ar_2COCl , $CHCl_3$; (viii) CF_3COOH , CH_2Cl_2 ; for the meaning of Ar_1 and Ar_2 , see Table 1.

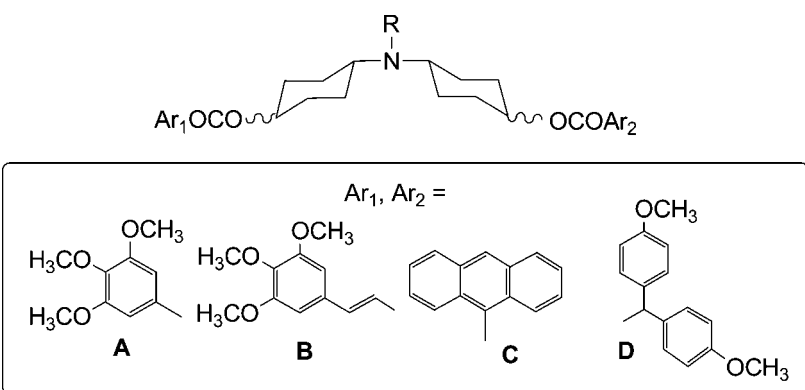
a matter of fact, K562 is a human leukemia cell line, established from a patient with a chronic myelogenous leukemia in blast transformation.⁴² K562/DOX cells resistant to doxorubicin express a unique membrane glycoprotein with a molecular mass of 180000 Da.⁴³ We measured the uptake of THP-adriamycin (pirarubicin) by continuous spectrofluorometric signal of the anthracycline at 590 nm ($\lambda_{ex} = 480$ nm) after incubation of the cells, following the protocols reported in previous papers.^{38,44–46} Pgp-blocking activity is described by (i) α , which represents the fold increase in the nuclear concentration of pirarubicin in the presence of the Pgp inhibitor and varies between 0 (in the absence of the inhibitor) and 1 (when the amount of pirarubicin in resistant cells is the same as in sensitive cells); (ii) α_{max} , which expresses the efficacy of the Pgp inhibitor and is the maximum increase that can be obtained in the nuclear concentration of pirarubicin in resistant cells with a given compound; and (iii)

$[I]_{0.5}$, which measures the potency of the inhibitor and represents the concentration that causes a half-maximal increase ($\alpha = 0.5$) in nuclear concentration of pirarubicin (see Table 1).

Even if binding experiments on Pgp were not performed, this test indicates that the compounds inhibit the Pgp-operated extrusion of the reporter molecule pirarubicin, as does the reference molecule verapamil. The molecules studied lack any detectable cytotoxicity at the doses used in the test.

Effects on ATPase Activity. ATP binding and hydrolysis are critical for efflux pump function, although it is still a matter of debate whether ATP hydrolysis is required for driving the substrate across the membrane or for resetting the transporter to the starting position or for both.^{47,48} Nevertheless, studies of the effects of MDR modulators on ATPase activity of the ABC transporter family are considered useful to get insight into the action mechanisms of these drugs. The effects of some of the

Table 1. MDR-Reverting Activity of Compounds 3–10



compd	structure ^a	R	Ar ₁	Ar ₂	[I] _{0.5} μM ^b	α _{max} ^c
1	I	CH ₃	A	B	0.60 ± 0.15 ^d	0.90
2	I	CH ₃	A	C	0.28 ± 0.05 ^e	0.71
3a (cis/trans)	II	CH ₃	A	B	0.092 ± 0.015	0.85
3b (trans/trans)	II	CH ₃	A	B	0.32 ± 0.10	0.81
3c (cis/cis)	II	CH ₃	A	B	0.03 ± 0.01	0.80
3d (trans/cis)	II	CH ₃	A	B	0.012 ± 0.001	0.98
4a (cis/trans)	II	CH ₃	A	C	0.30 ± 0.06	0.95
4b (trans/trans)	II	CH ₃	A	C	0.30 ± 0.06	0.88
4c (cis/cis)	II	CH ₃	A	C	0.18 ± 0.03	0.79
4d (trans/cis)	II	CH ₃	A	C	0.16 ± 0.06	0.78
5a (cis/trans)	II	CH ₃	B	C	0.14 ± 0.02	0.67
5b (trans/trans)	II	CH ₃	B	C	0.15 ± 0.01	0.60
5c (cis/cis)	II	CH ₃	B	C	0.17 ± 0.08 ^f	0.38
5d (trans/cis)	II	CH ₃	B	C	0.16 ± 0.07 ^f	0.40
6a (cis/trans)	II	CH ₃	B	D	0.19 ± 0.03 ^f	0.39
6b (trans/trans)	II	CH ₃	B	D	0.12 ± 0.06 ^f	0.46
6c (cis/cis)	II	CH ₃	B	D	1.19 ± 0.4	0.52
6d (trans/cis)	II	CH ₃	B	D	0.13 ± 0.08 ^f	0.44
7a (cis/trans)	II	CH ₃	A	A	0.13 ± 0.06	0.61
7b (trans/trans)	II	CH ₃	A	A	0.35 ± 0.11	0.73
7c (cis/cis)	II	CH ₃	A	A	2.0 ± 0.6	0.98
8a (cis/trans)	II	CH ₃	B	B	0.12 ± 0.04 ^f	0.36
8b (trans/trans)	II	CH ₃	B	B	0.11 ± 0.03 ^f	0.47
8c (cis/cis)	II	CH ₃	B	B	1.13 ± 0.4 ^f	0.44
9a/b (cis/trans + trans/trans)	II	CH ₃	C	C	0.70 ± 0.14 ^g	0.50
10a/b (cis/trans + trans/trans)	II	H	A	B	3.30 ± 0.06	0.70
verapamil					1.60 ± 0.3	0.70
MM36					0.05 ± 0.01 ^h	0.70

^a See Chart 1. ^b Concentration of the inhibitor that causes a 50% increase in nuclear concentration of pirarubicin ($\alpha = 0.5$). ^c Efficacy of MDR-modulator: maximum increase that can be obtained in the nuclear concentration of pirarubicin in resistant cells. ^d See ref 26. ^e See ref 30. ^f Concentration of the inhibitor that causes a 30% increase in nuclear concentration of pirarubicin ($\alpha = 0.3$). ^g Concentration of the inhibitor that causes a 40% increase in nuclear concentration of pirarubicin ($\alpha = 0.4$). ^h See ref 46.

synthesized compounds on pump ATPase activity of brush border plasma membrane vesicles, prepared from homogenates of rat small intestine mucosa, were evaluated.⁴⁹ In plasma membrane vesicles, as shown in Figure S1 (Supporting Information), MRP1, MRP2, and Pgp were present in detectable amounts. On the assumption of the existence of multiple binding sites on Pgp and sister proteins, both basal ATPase activity and ATPase activity stimulated by the substrate verapamil were assayed in the absence or in the presence of MDR-inhibitors.

Effects on Doxorubicin Cytotoxicity. The assessment of the ability of a compound to enhance the growth inhibitory effects of doxorubicin in tumor cell lines showing MDR due to Pgp overexpression has also been proved useful in the quantification and characterization of MDR reversal by modulators of the MDR phenotype. Comparisons are made between the effects on the sensitivity to doxorubicin in doxorubicin-resistant cells in the presence and in the absence of an inhibitor.

The reversal effects of compounds 3a–d and 4a–d on the MDR phenotype were investigated on doxorubicin-resistant erythroleukemia K562 cells (K562/DOX) overexpressing only

Pgp.^{40,41} Test compounds were evaluated for their intrinsic cytotoxicity and MDR-reversal activity in vitro using the MTT (3-(4,5-dimethylthiazolyl-2)-2,5-diphenyltetrazolium bromide) assay.⁵⁰

The IC₅₀ drug concentrations resulting in a 50% reduction in the conversion of MTT in drug-treated cells compared to untreated control cells were calculated from plotted results. The potency of MDR reversal was expressed by the reversal-fold (RF) values, obtained by dividing the doxorubicin IC₅₀ values of K562 and K562/DOX cells in the absence of modulators by those in the same cells in the presence of modulators (see Table 2). All results are presented as mean ± SE, and statistical analysis was performed using one-way Anova test and Bonferroni's multiple comparison test (GraphPad Prism software, Inc. CA).

Results

Modulation of Pirarubicin Uptake. The results obtained on doxorubicin-resistant erythroleukemia K562 cells are reported in Table 1, together with those of two parent linear compounds

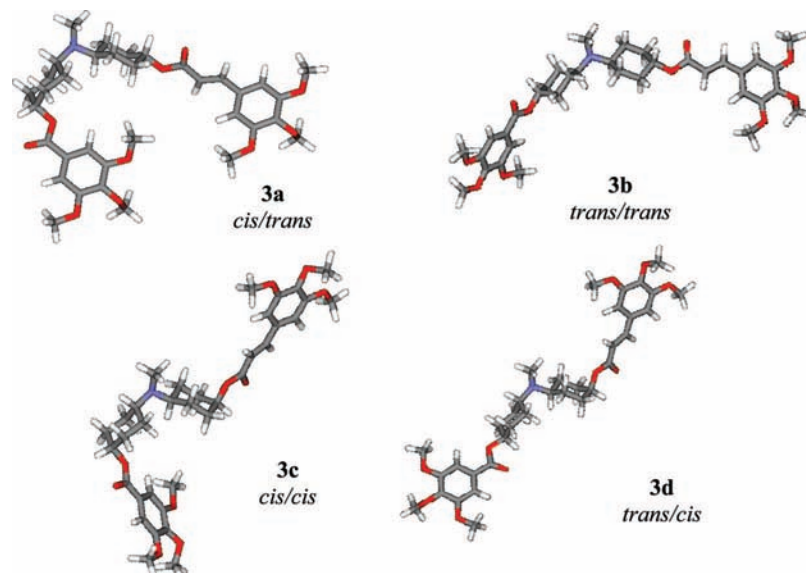


Figure 1. Lowest-energy conformations of **3a**, **3b**, **3c**, and **3d**. The compounds were built within Spartan '04 (wave function) and minimized using semiempirical methods (AM1). A conformational analysis was performed starting from the cyclohexane rings built in the chair conformation and by rotating each flexible bond. The groups on the *trans*-substituted cyclohexane ring have been calculated only in the diequatorial position. For **3a** and **3c**, both *cis* isomers (i.e., those having the ester and amino groups in axial/equatorial position) have been calculated: it was found that lower energy is always associated with the conformer showing the trimethoxybenzoate group axial and the methylcyclohexylamino group equatorial, with ΔE values changing according to the different conformation on the rest of the molecules (2–5 kcal/mol). Fairly similar results were obtained with the isomers of compounds **4–8**.

Table 2. Effects of Studied MDR-Reversing Agents on Doxorubicin Cytotoxicity in K562 Cells and K562/DOX Cells^a

compd	K562		K562/DOX	
	IC ₅₀ (μ M) ^b	RF ^c	IC ₅₀ (μ M) ^b	RF ^c
DOX	0.032 ± 0.002	1.0	2.84 ± 0.047	1.0
DOX + 3a (0.092 μ M) ^d	nd	nd	2.77 ± 0.24	1.0
DOX + 3a (1 μ M)	0.046 ± 0.011	0.7	0.37 ± 0.13 ^e	7.7
DOX + 3a (3 μ M)	0.069 ± 0.013	0.5	0.29 ± 0.06 ^e	9.8
DOX + 3b (0.32 μ M) ^d	nd	nd	1.26 ± 0.082 ^f	2.3
DOX + 3b (1 μ M)	0.048 ± 0.01	0.7	0.31 ± 0.03 ^e	9.2
DOX + 3b (3 μ M)	0.038 ± 0.013	0.8	0.21 ± 0.03 ^e	13.5
DOX + 3c (0.03 μ M) ^d	nd	nd	1.39 ± 0.13	2.0
DOX + 3c (1 μ M)	0.045 ± 0.015	0.7	0.29 ± 0.06 ^e	9.8
DOX + 3c (3 μ M)	0.046 ± 0.013	0.7	0.16 ± 0.02 ^e	17.8
DOX + 3d (0.01 μ M) ^d	nd	nd	0.77 ± 0.16 ^e	3.7
DOX + 3d (1 μ M)	0.050 ± 0.009	0.6	0.14 ± 0.03 ^e	20.3
DOX + 3d (3 μ M)	0.037 ± 0.008	0.9	0.078 ± 0.006 ^e	36.4
DOX + 4a (0.3 μ M) ^d	nd	nd	2.23 ± 0.29	1.3
DOX + 4a (1 μ M)	0.027 ± 0.005	1.2	0.57 ± 0.06 ^e	5.0
DOX + 4a (3 μ M)	0.019	1.7	0.25 ± 0.044 ^e	11.4
DOX + 4b (0.3 μ M) ^d	nd	nd	2.33 ± 0.3 ^e	1.2
DOX + 4b (1 μ M)	0.048 ± 0.001	0.7	0.34 ± 0.065 ^e	8.4
DOX + 4b (3 μ M)	0.023	1.4	0.21 ± 0.036 ^e	13.5
DOX + 4c (0.18 μ M) ^d	nd	nd	0.52 ± 0.093 ^e	5.5
DOX + 4c (1 μ M)	0.025 ± 0.001	1.3	0.17 ± 0.032 ^e	16.7
DOX + 4c (3 μ M)	0.0069	4.6	0.14 ± 0.032 ^e	20.3
DOX + 4d (0.16 μ M) ^d	nd	nd	1.75 ± 0.18 ^e	1.6
DOX + 4d (1 μ M)	0.028 ± 0.008	1.1	0.2 ± 0.014 ^e	14.2
DOX + 4d (3 μ M)	0.011	2.9	0.14 ± 0.036 ^e	20.3
DOX + verapamil (1.6 μ M) ^d	nd	nd	0.84 ^f	3.4
DOX + verapamil (1 μ M)	0.048 ± 0.008	0.7	1.7 ± 0.09 ^e	1.7
DOX + verapamil (3 μ M)	0.058 ± 0.004	0.6	0.68 ± 0.05 ^e	4.2

^a nd = not determined. ^b Mean ± SE of at least three determinations or mean of two determinations performed with quadruplicate cultures at each drug concentration tested and measured as described in Experimental section. ^c Reversal fold of MDR was determined by dividing the IC₅₀ values of doxorubicin of K562 and K562/DOX cells in the absence of modulators by those in the presence of modulators. ^d [I]_{0.5} value which measures the potency of the inhibitor and represents the concentration that causes a half-maximal increase ($\alpha = 0.5$) in nuclear concentration of pirarubicin. ^e $p < 0.001$ of IC₅₀ of treated K562/DOX cells vs control cells (K562/DOX cells treated with doxorubicin only). Where not specified the IC₅₀ values of treated K562 and K562/DOX cells are not significantly different compared to control cells (K562 and K562/DOX cells treated with doxorubicin only). ^f $p < 0.01$ of IC₅₀ of treated K562/DOX cells vs control cells (K562/DOX cells treated with doxorubicin only). Where not specified the IC₅₀ values of treated K562 and K562/DOX cells are not significantly different compared to control cells (K562 and K562/DOX cells treated with doxorubicin only).

1²⁶ and **2³⁰** (Structure I, Chart 1) and of MM36, the most potent compound that we have found in previous studies,⁴⁶ and verapamil used as reference compounds.

Except for the mixture **10a/b**, the new molecules are all able to modulate the activity of Pgp, being more potent than the standard reference compound verapamil. Their potencies range

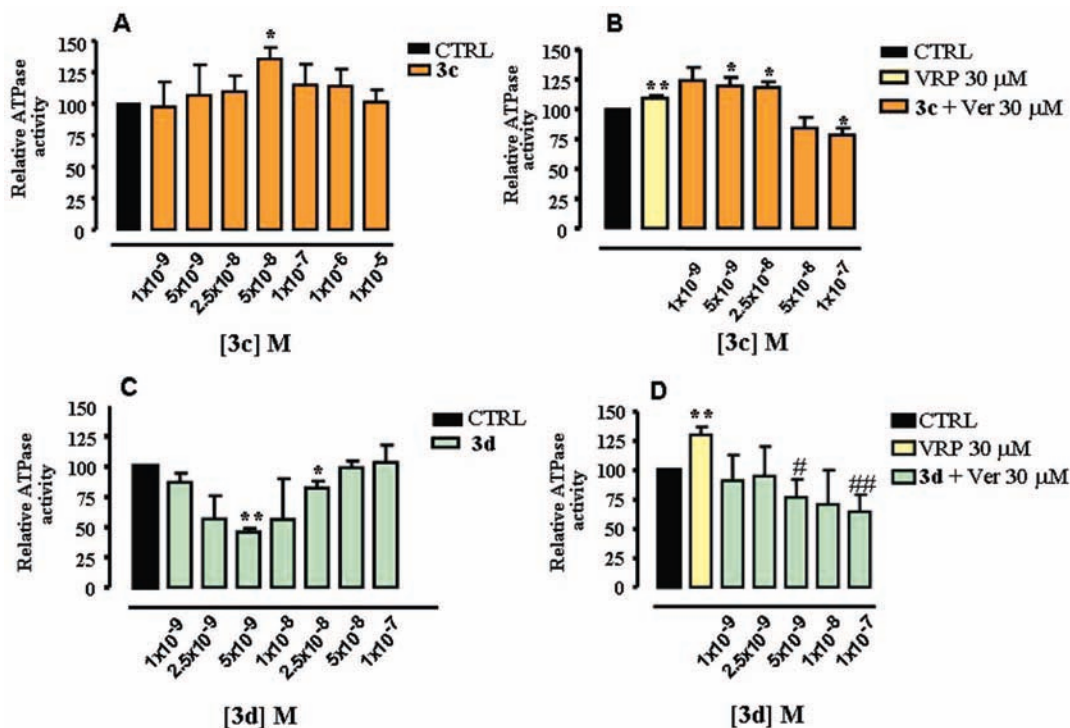


Figure 2. Effects of **3c** and **3d** on basal (A,C) and verapamil-stimulated (B,D) ATPase activity. Under control conditions (no drug added, CTRL) basal ATPase activity was considered to be 100%. * $p < 0.05$; ** $p < 0.01$ one sample t test vs CTRL ($n = 3-5$). # $p < 0.05$; ## $p < 0.01$ one sample t test vs verapamil ($n = 3-5$).

from low nanomolar (compounds **3a**, **3c**, **3d**) to micromolar values (**6c**, **7c**, **8c**), the remaining compounds being in the high nanomolar range. Some compounds (**3d**, **4a**, **7c**) show nearly complete reversal of MDR (α_{\max} close to 1), while a few show very low α_{\max} (< 0.5) and seem unable to achieve a significant control of MDR. In these cases (**5c**, **5d**, **6a**, **6b**, **6d**, **8a**, **8b**, **8c**, **9a/b**), the $[I]_{0.5}$ could not be evaluated and potency was measured at the lower value of α reported in Table 1. Confirming previously found structure–activity relationships,²⁶ *N*-methyl derivatives seem more active than the corresponding secondary amines as it can be seen comparing **3a** and **3b** with **10a/b** ($[I]_{0.5} = 0.092 \mu\text{M}$, and $0.32 \mu\text{M}$ and $3.30 \mu\text{M}$, respectively).

Effects on ATPase Activity. The effect of isomers **3a–d** on ATPase activity was evaluated. In the assay protocol used, ATPase activity was fully inhibited by low micromolar concentrations of Na_3VO_4 , thus indicating that it was totally ascribable to Pgp or MRPs.⁵¹ Verapamil stimulated the basal ATPase activity, thus behaving like a substrate for the pumps.

As reported in panel A of Figure 2, compound **3c** gave a typical bell-shaped concentration–activation curve with 5×10^{-8} M maximum effective concentration, thus behaving like a Pgp ATPase substrate. Moreover, this isomer showed a bimodal effect on 30 μM verapamil-stimulated ATPase activity (Figure 2, panel B). In fact, this activity was stimulated at concentrations $\leq 2.5 \times 10^{-8}$ M, while it was inhibited at higher concentrations.

Compound **3d** inhibited, with a typical bell-shaped concentration–inhibition curve, the basal ATPase activity, maximal inhibition (about 55%) being achieved at 5×10^{-9} M concentration (Figure 2, panel C). At higher concentrations, the inhibition was reversed up to values comparable to those of control preparations. Moreover, at concentrations $\leq 5 \times 10^{-9}$ M, **3d** fully antagonized the portion of ATPase activity stimulated by verapamil (Figure 2, panel D), thus indicating a clear antagonism toward verapamil activation. Compounds **3a** and **3b** did not exert significant effects (data not shown).

Effects on Doxorubicin Cytotoxicity. The ability of compounds **3a–d** and **4a–d** to reverse drug resistance of K562/DOX cells was examined in comparison to verapamil.

Preliminarily, it was checked whether compounds **3a–d**, **4a–d** and verapamil alone exerted cytotoxic effects on K562 and K562/DOX cells. In both cell lines, isomers of compounds **3** and **4** and verapamil had an intrinsic toxicity not exceeding 20% at all concentrations tested ($[I]_{0.5}$, 1 μM and 3 μM) with the exception of isomers **4c** and **4d**, which presented a 35% cell growth inhibition at 3 μM concentration (data not shown).

The effects on the reversion of doxorubicin resistance were examined after the cells were incubated at 37 °C for 72 h at $[I]_{0.5}$ concentration of each compound, which represents the concentration that causes a half-maximal increase in nuclear concentration of pirarubicin and at 1 and 3 μM concentrations. Results are reported in Table 2.

At the $[I]_{0.5}$ concentration, isomer **3a** did not display any drug resistance reversal activity in K562/DOX cells. At the same concentration, isomers **3b** and **3c** significantly reverted doxorubicin resistance in these cells by a factor (RF) of about 2. The most relevant and significant effect was obtained with isomer **3d**, which reverted doxorubicin resistance in K562/DOX cells by a RF of 3.7. At the higher concentrations (1 and 3 μM) all isomers (**3a–d**) were able to markedly reverse doxorubicin resistance (RF values ranging from 7.7 to 36.4). Also at these concentrations isomer **3d** was the most active, isomers **3b** and **3c** displayed intermediate activity, and isomer **3a** was the least active.

Isomers **4a** and **4b** at the $[I]_{0.5}$ dose did not reverse doxorubicin resistance in K562/DOX cells showing RF values slightly above 1. At higher concentrations (1 and 3 μM), they exerted marked reversal effects on drug-induced cell growth inhibition (RF values ranging from 5.0 to 13.5). At $[I]_{0.5}$, **4c** was a potent resistance reversal agent in this cell line (RF value 5.5), while isomer **4d** displayed borderline reversal activity (RF value 1.6). At the higher concentrations tested, isomers **4c** and

4d increased significantly cell growth inhibitory effects induced by doxorubicin and RF values ranging from 14.2 to 20.3 were observed. While at 1 μM , these interactions may be attributed to specific modulatory effects on Pgp function, at 3 μM , a direct cytotoxic effect of studied isomers may have affected experimental results.

When comparing reversal effects of the new compounds and verapamil at $[\text{I}]_{0.5}$, similar reversal activities were observed for isomers **3d**, **4c**, and verapamil. At higher concentrations (1 and 3 μM), all isomers were clearly more effective in enhancing the cell growth inhibitory effects of doxorubicin as compared to equimolar verapamil concentrations.

When the effects of the new compounds were examined on parental doxorubicin sensitive K562 cells at the concentrations of 1 and 3 μM , statistically not significant differences in IC_{50} were observed for isomers **3a–d** (RF values ranging from 0.5 to 0.9). When isomers **4a–d** were used in combination with doxorubicin, increased cytotoxic effects were usually observed. They were modest at 1 μM and more pronounced, albeit not significant, at 3 μM .

Discussion

Modulation of Pirarubicin Uptake and SARs. As stated above, we have used pirarubicin uptake in doxorubicin-resistant erythroleukemia K562 cells as a screening assay to evaluate the interaction of our compounds with Pgp; as a consequence, we will rely on the results obtained in this test to draw some structure–activity relationships for the whole series. The results reported in Table 1 show that, as it is usual when applying the frozen analogue approach, the compounds of the series show a quite different pharmacological behavior that spans from the excellent activity of the isomers of set **3** to the poor performance of those of set **8**. Very likely, this is the consequence of two concurrent properties: isomeric geometry and the nature of the aryl moieties. In each isomer of the series, the scaffold is fairly rigid and the aryl moieties are forced into discrete positions with limited conformational freedom, something that may favor or disfavor the affinity for the binding site depending on the nature of the aromatic moieties.

The best combination of these properties is apparently that of compound **3d**, the most potent and efficacious member of the series, that combines a *trans/cis* geometry with 3,4,5-trimethoxybenzoic and *trans*-3,4,5-trimethoxycinnamic aryl moieties. The other isomers of the set (**3a**, **3b**, **3c**) are also potent and efficacious modulators of Pgp, being more active than the corresponding linear compound **1**,²⁶ the differences in their potency and efficacy reflecting their different geometry. A similar situation is found in the set of isomers **4**: even in this case the *trans/cis* isomer (**4d**) is the most active, yet some ten times less than **3d**. In this case, restriction of conformational freedom does not pay, and the four isomers of **4** maintain the activity of the corresponding linear compound **2**.³⁰ Clearly, because the isomers of set **4** have the same geometrical features of those of set **3**, these differences have to be ascribed to the anthracene moiety. Apparently, as the conformational freedom is reduced, the nature of the aromatic moieties gains importance, a consequence that is in accord with our original hypothesis that flexible molecules can more easily find the most productive interaction with the recognition site. As a matter of fact, the anthracene moiety (set **4** and **5**) that produced very effective Pgp inhibitors in flexible molecules (see compound **2**, but also the analogous compounds reported in the previous exploratory work²⁶) appears to be less effective when inserted in less flexible structures.

If the atomic structure of Pgp were available, we could check the soundness of this hypothesis and improve the affinity of the compounds of the series. Unfortunately, only a few homology models^{12–14} developed after the structure of homologous bacterial transporters and not very useful for this purpose, are known. Therefore, we had to rely on the old trial and error approach, which, so far, has yielded disappointing results. For instance, the attempt to improve the fitting of set **5** by restoring the conformational freedom of the two phenyl rings of anthracene (set **6**) afforded nearly less potent and less efficacious compounds. Disappointing results were also obtained with the series of compounds substituted with identical aromatic moieties (sets **7** and **8**).

Pharmacological Profiling of Most Potent Compounds.

The ATPase modulation of the isomers of set **3** was evaluated: the test confirmed the activity and the high potency revealed by the pirarubicin uptake assay. Also, in this test, the isomers behave in a quite different way: compounds **3a** and **3b** did not exert significant effects; compound **3c** gave a typical bell-shaped activation curve with a maximum at 5×10^{-8} M, while **3d** inhibited the basal ATPase activity, maximal inhibition (about 55%) being achieved at a 5×10^{-9} M concentration. When ATPase activity was stimulated with 30 μM verapamil, compound **3c** increased enzymatic activity up to 2.5×10^{-8} M but inhibited it at higher concentrations, whereas compound **3d** fully antagonized verapamil-stimulated enzymatic activity at 5×10^{-9} M concentration. These results show that of the four isomers tested, **3c** behaves like a substrate while **3d** behaves like an inhibitor/substrate of ATPase activity.³³

The results of cytotoxicity tests demonstrated that isomers **3d**, **4c**, and **4d** significantly enhanced doxorubicin sensitivity of K562/DOX cells. While intrinsic cytotoxicity of isomer **3d** was limited (<20%), isomers **4c** and **4d** at high concentration (3 μM) induced cell growth inhibition of both K562/DOX and K562 cells (about 35%). This suggests that the effects of isomers **3d** on doxorubicin cytotoxicity may be specifically mediated by Pgp interactions in an overexpressing cell phenotype, while those of **4c** and **4d** may be partially not specific. Lack of isomer **3d** effects on the sensitivity to doxorubicin of the sensitive K562 cell line also suggests specificity.

As far as the selectivity of our compounds against different types of ABC transporters is concerned, the results of intestine vesicles would suggest that they may be active also on MRP1 and sister proteins. On these bases, a novel ongoing investigation has been started and the results will be disclosed in due time.

In conclusion, applying the frozen analogue approach to a series of very flexible MDR reverters²⁶ has led us to identify a new series of drugs that show very interesting MDR-reverting properties. Among them, compound **3d**, which consistently shows low nanomolar potency and high efficacy in all the tests used, appears as a new pharmacological tool for Pgp studies and a promising lead for the development of potent, efficient, and safe MDR reverters.

Experimental Section

Chemistry. All melting points were taken on a Büchi apparatus and are uncorrected. Infrared spectra were recorded with a Perkin-Elmer 681 or a Perkin-Elmer Spectrum RX I FT-IR spectrophotometer. ¹H NMR spectra were recorded on Bruker Avance 400 spectrometer. Chromatographic separations were performed on a silica gel column by flash chromatography (Kieselgel 40, 0.040–0.063 mm; Merck). Yields are given after purification, unless stated otherwise. Where analyses are indicated by symbols, the analytical results are within $\pm 0.4\%$ of the theoretical values. We have chosen to perform and report only the combustion analyses of final

compounds. The identity and purity of the intermediates was ascertained through IR, ^1H NMR, and TLC chromatography. When reactions were performed in anhydrous conditions, the mixtures were maintained under nitrogen.

Compounds were named following IUPAC rules as applied by Beilstein-Institut AutoNom 2000 4.01.305, a software for systematic names in organic chemistry.

3,4,5-Trimethoxybenzoic Acid 4-Oxocyclohexyl Ester (11). 3,4,5-Trimethoxybenzoic acid (710 mg, 3.34 mmol) was transformed into the acyl chloride by reaction with SOCl_2 (2 equiv) in 5 mL CHCl_3 (free of EtOH) at 60 °C for 4 h. The reaction mixture was cooled to room temperature and the solvent was removed under reduced pressure. The acyl chloride obtained was dissolved in CHCl_3 (free of EtOH), and 4-hydroxycyclohexanone³⁴ (0.23 g, 2.00 mmol) was added. The reaction mixture was heated to 60 °C for 8 h and then cooled to room temperature, treated with CH_2Cl_2 , and the organic layer washed with 10% NaOH solution. After drying with Na_2SO_4 , the solvent was removed under reduced pressure and the residue purified by flash chromatography using cyclohexane/ethyl acetate (7:3) as eluting system. The title compound (420 mg, 68% yield) was obtained. IR (neat): ν 1712 (CO), 1694 (CO) cm^{-1} . ^1H NMR (CDCl_3): δ 7.25 (s, 2H, aromatics); 5.41–5.32 (m, 1H, CHO); 3.85 (s, 9H, 3OCH₃); 2.57–2.53 (m, 2H, CH₂); 2.51–2.40 (m, 2H, CH₂); 2.21–2.16 (m, 4H, 2CH₂) ppm.

Compounds **12** and **13** were obtained in the same way from *trans*-3-(3,4,5-trimethoxyphenyl)-acryloyl chloride or anthracene-9-carbonyl chloride, respectively. Their IR and ^1H NMR spectra are consistent with the proposed structures.

3,4,5-Trimethoxybenzoic Acid 4-(4-Hydroxycyclohexylamino)cyclohexyl Ester (14a/b). A mixture of compound **11** (420 mg, 1.36 mmol), *trans*-4-aminocyclohexanol (160 mg, 1.36 mmol), and titanium(IV) isopropoxide (0.44 mL, 1.36 mmol) was stirred at room temperature. After 3 h, absolute ethanol (2.5 mL) and NaBH_3CN (170 mg, 1.79 mmol) were added and the solution was stirred for 20 h. Water (10 mL) was added, the organic solvent was removed under reduced pressure, to then the mixture was treated with CH_2Cl_2 and the organic layer washed with a saturated solution of NaHCO_3 . After drying with Na_2SO_4 , the solvent was removed under reduced pressure and the residue purified by flash chromatography using $\text{CHCl}_3/\text{MeOH}$ (9:1) as eluting system. The title compound (410 mg, 74% yield) as a mixture of *cis/trans* and *trans/trans* isomers was obtained as a white solid; mp: 45–47 °C. IR (neat): ν 3350 (OH and NH); 1723 (CO) cm^{-1} . ^1H NMR (CDCl_3): δ 7.27 (s, 2H, aromatics); 5.12 (bs, 0.5H, CHO); 4.92 (tt, $J = 10.8$ Hz, $J = 4.4$ Hz, 0.5H, CHO); 3.87 (s, 9H, 3OCH₃); 3.70–3.48 (m, 1H, CHOH); 2.73–2.49 (m, 2H, 2NCH); 2.20–1.01 (m, 18H, 8CH₂, OH and NH) ppm.

Compounds **15a/b** and **16a/b** were obtained in the same way from **12** and **13**, respectively. Compounds **14c/d** and **15c/d** were obtained in the same way from **11** and **12**, respectively, using *cis*-4-aminocyclohexanol.³⁵ Their IR and ^1H NMR spectra are consistent with the proposed structures.

***cis/trans*-3,4,5-Trimethoxybenzoic Acid 4-(4-Hydroxycyclohexylamino)cyclohexyl Ester (14a) and *trans/trans*-3,4,5-Trimethoxybenzoic Acid 4-(4-Hydroxycyclohexylamino)cyclohexyl Ester (14b).** Flash chromatography of 240 mg of compound **14a/b**, as an approximately 50/50 mixture of *cis/trans* and *trans/trans* isomers, afforded the two isomers *cis/trans* and *trans/trans* (**14a** and **14b**) using $\text{CHCl}_3/\text{MeOH}/\text{NH}_3$ (90:10:0.5) as eluting system.

***cis/trans* 14a.** Yield 90 mg as a colorless oil; $R_f = 0.50$. IR (neat): ν 3350 (OH and NH); 1723 (CO) cm^{-1} . ^1H NMR (CDCl_3): δ 7.27 (s, 2H, aromatics), 5.12 (bs, 1H, CHO), 3.91 (s, 9H, 3OCH₃), 3.60 (tt, $J = 10.6$ Hz, $J = 4.0$ Hz, 1H, CHOH), 2.71 (tt, $J = 9.6$ Hz, $J = 3.2$ Hz, 1H, NCH), 2.59 (tt, $J = 10.8$ Hz, $J = 3.6$ Hz, 1H, NCH), 2.06–1.10 (m, 18H, 8CH₂, OH and NH) ppm.

***trans/trans* 14b.** Yield 70 mg as a white solid (mp: 127–128 °C); $R_f = 0.43$. IR (neat): ν 3350 (OH and NH); 1723 (CO) cm^{-1} . ^1H NMR (CDCl_3): δ 7.27 (s, 2H, aromatics), 4.92 (tt, $J = 10.8$ Hz, $J = 4.4$ Hz, 1H, CHO), 3.90 (s, 9H, 3OCH₃), 3.62 (tt, $J = 10.6$ Hz, $J = 4.0$ Hz, 1H, CHOH), 2.66 (t, $J = 11.2$ Hz, 1H, NCH),

2.60 (t, $J = 10.8$ Hz, 1H, NCH), 2.15–1.13 (m, 18H, 8CH₂, OH and NH) ppm.

The two isomers **15a** and **15b** were obtained in the same way by chromatographic separation of the approximately 50/50 mixture of *cis/trans* and *trans/trans* isomers **15a/b** (1.08 g).

***cis/trans* 15a.** Yield 350 mg as a colorless oil; $R_f = 0.38$. IR (neat): ν 3350 (OH e NH); 1708 (CO) cm^{-1} . ^1H NMR (CDCl_3): δ 7.58 (d, 1H, CH=CH, $J = 16.0$ Hz), 6.75 (s, 2H, aromatics), 6.32 (d, 1H, CH=CH, $J = 16.0$ Hz), 5.08 (bs, 1H, CHO), 3.88 (s, 6H, 2OCH₃), 3.86 (s, 3H, OCH₃), 3.63–3.53 (m, 1H, CHOH), 2.75–2.65 (m, 1H, NCH), 2.63–2.54 (m, 1H, NCH), 2.01–1.90 (m, 6H, 3CH₂), 1.77–1.69 (m, 2H, CH₂), 1.63–1.48 (m, 4H, 2CH₂), 1.36–1.23 (m, 2H, CH₂), 1.21–1.06 (m, 2H, CH₂) ppm.

***trans/trans* 15b.** Yield 200 mg as a white solid (mp: 168–170 °C); $R_f = 0.32$. IR (neat): ν 3350 (OH e NH); 1708 (CO) cm^{-1} . ^1H NMR (CDCl_3): δ 7.57 (d, 1H, CH=CH, $J = 16.0$ Hz), 6.75 (s, 2H, aromatics), 6.32 (d, 1H, CH=CH, $J = 16.0$ Hz), 4.82 (tt, 1H, CHO, $J = 10.8$ Hz, $J = 4.4$ Hz), 3.87 (s, 9H, 3OCH₃), 3.62 (tt, 1H, CHO, $J = 10.8$ Hz, $J = 4.0$ Hz), 2.69–2.59 (m, 2H, 2NCH), 2.14–1.93 (m, 8H, 4CH₂), 1.52–1.40 (m, 2H, CH₂), 1.39–1.13 (m, 6H, 3CH₂) ppm.

The two isomers **14c** and **14d** were obtained in the same way by chromatographic separation of the approximately 50/50 mixture of *cis/cis* and *trans/cis* isomers **14c/d** (0.72 g).

***cis/cis* 14c.** Yield 200 mg as a light-yellow oil; $R_f = 0.52$. IR (neat): ν 3350 (OH and NH); 1723 (CO) cm^{-1} . ^1H NMR (CDCl_3): δ 7.31 (s, 2H, aromatics), 5.15 (bs, 1H, CHO), 3.94 (bs, 1H, CHOH), 3.90 (m, 9H, 3OCH₃), 2.81–2.70 (m, 2H, 2NCH), 2.06–1.98 (m, 2H, CH₂), 1.83–1.51 (m, 14H, 7CH₂) ppm.

***trans/cis* 14d.** Yield 150 mg as a light-yellow oil; $R_f = 0.45$. IR (neat): ν 3350 (OH and NH); 1723 (CO) cm^{-1} . ^1H NMR (CDCl_3): δ 7.27 (s, 2H, aromatics), 4.93 (tt, $J = 10.8$ Hz, $J = 4.4$ Hz, 1H, CHO), 3.94 (bs, 1H, CHOH), 3.90 (m, 9H, 3OCH₃), 2.80–2.72 (m, 2H, 2NCH), 2.18–2.11 (m, 2H, CH₂), 2.08–2.01 (m, 2H, CH₂), 1.83–1.34 (m, 12H, 6CH₂) ppm.

The two isomers **15c** and **15d**, were obtained in the same way by chromatographic separation of the approximately 50/50 mixture of *cis/cis* and *trans/cis* isomers **15c/d** (1.70 g).

***cis/cis* 15c.** Yield 500 mg as a light-pink oil; $R_f = 0.38$. IR (neat): ν 3350 (OH e NH); 1708 (CO) cm^{-1} . ^1H NMR (CDCl_3): δ 7.61 (d, 1H, CH=CH, $J = 16.0$ Hz), 6.78 (s, 2H, aromatics), 6.33 (d, 1H, CH=CH, $J = 16.0$ Hz), 5.11–5.07 (m, 1H, CHO), 3.92–3.88 (m, 7H, 2OCH₃ + CHO), 3.86 (s, 3H, OCH₃), 2.82–2.70 (m, 2H, 2NCH), 2.02–1.92 (m, 2H, CH₂), 1.81–1.51 (m, 14H, 7CH₂) ppm.

***trans/cis* 15d.** Yield 280 mg as a light-pink oil; $R_f = 0.33$. IR (neat): ν 3350 (OH e NH); 1708 (CO) cm^{-1} . ^1H NMR (CDCl_3): δ 7.56 (d, 1H, CH=CH, $J = 16.0$ Hz), 6.74 (s, 2H, aromatics), 6.31 (d, 1H, CH=CH, $J = 16.0$ Hz), 4.82 (tt, 1H, CHO, $J = 10.8$ Hz, $J = 4.4$ Hz), 3.95–3.89 (m, 1H, CHO), 3.88 (s, 6H, 2OCH₃), 3.86 (s, 3H, OCH₃), 2.76–2.64 (m, 2H, 2NCH), 2.14–2.06 (m, 2H, CH₂), 2.05–1.95 (m, 2H, CH₂), 1.80–1.25 (m, 12H, 6CH₂) ppm.

***cis/trans*-3,4,5-Trimethoxybenzoic Acid 4-[(4-Hydroxycyclohexyl)methylamino]cyclohexyl Ester (17a).** To a solution of 410 mg (1.0 mmol) of **14a** in 1 mL of absolute ethanol, 0.66 mL of HCOOH and 0.38 mL of HCHO were added. The mixture was heated to 80 °C for 4 h and concentrated in vacuo. The residue was then dissolved in CH_2Cl_2 , and the organic layer was washed with a saturated solution of NaHCO_3 and with water. After drying with Na_2SO_4 , the solvent was removed under reduced pressure. The crude product was then purified by flash chromatography using $\text{CH}_2\text{Cl}_2/\text{abs EtOH}/\text{ethyl ether}/\text{petroleum ether}/\text{NH}_4\text{OH}$ 360:180:360:900:9.9 as eluting system. Compound **17a** was obtained as an oil (250 mg, 59% yield). IR (neat): ν 3370 (OH); 1714 (CO) cm^{-1} . ^1H NMR (CDCl_3): δ 7.31 (s, 2H, aromatics), 5.18 (bs, 1H, CHO), 3.90 (s, 9H, 3OCH₃), 3.61–3.51 (m, 1H, CHOH), 2.69–2.51 (m, 2H, 2NCH), 2.26 (s, 3H, NCH₃), 2.20–1.18 (m, 17H, 8CH₂, and OH) ppm.

Compounds **17b**, **17c**, and **17d** were obtained in the same way from **14b**, **14c**, and **14d**, respectively.

***trans/trans* 17b.** IR (neat): ν 3370 (OH); 1714 (CO) cm^{-1} . ^1H NMR (CDCl_3): δ 7.28 (s, 2H, aromatics), 4.95–4.78 (m, 1H, CHO),

3.91 (s, 9H, 3OCH₃), 3.61–3.55 (m, 1H, CHOH), 2.70–2.50 (m, 2H, 2NCH), 2.27 (s, 3H, NCH₃), 2.20–1.18 (m, 17H, 8CH₂, and OH) ppm.

cis/cis 17c. IR (neat): ν 3370 (OH); 1714 (CO) cm⁻¹. ¹H NMR (CDCl₃): δ 7.32 (s, 2H, aromatics), 5.19 (bs, 1H, CHO), 3.96 (bs, 1H, CHOH), 3.90 (s, 9H, 3OCH₃), 2.79–2.62 (m, 2H, 2NCH), 2.33 (s, 3H, NCH₃), 2.18–2.05 (m, 2H, CH₂), 1.83–1.51 (m, 15H, 7CH₂, and OH) ppm.

trans/cis 17d. IR (neat): ν 3370 (OH); 1714 (CO) cm⁻¹. ¹H NMR (CDCl₃): δ 7.26 (s, 2H, aromatics), 4.93–4.81 (m, 1H, CHO), 3.97 (bs, 1H, CHOH), 3.89 (s, 9H, 3OCH₃), 2.77–2.56 (m, 2H, 2NCH), 2.31 (s, 3H, NCH₃), 2.21–2.13 (m, 2H, CH₂), 1.98–1.49 (m, 15H, 7CH₂, and OH) ppm.

Compounds **18a**, **18b**, **18c**, and **18d** were obtained in the same way from **15a**, **15b**, **15c**, and **15d**, respectively.

cis/trans 18a. ¹H NMR (CDCl₃): δ 7.61 (d, 1H, CH=CH, J = 16.0 Hz), 6.77 (s, 2H, aromatics), 6.35 (d, 1H, CH=CH, J = 16.0 Hz), 5.12–5.08 (m, 1H, CHO), 3.90 (s, 6H, 2OCH₃), 3.88 (s, 3H, OCH₃), 3.57 (tt, 1H, CHOH, J = 10.8 Hz, J = 4.0 Hz), 2.64–2.55 (m, 2H, 2NCH), 2.30 (s, 3H, NCH₃), 2.09–2.00 (m, 4H, 2CH₂), 1.89–1.30 (m, 12H, 6CH₂) ppm.

trans/trans 18b. ¹H NMR (CDCl₃): δ 7.56 (d, 1H, CH=CH, J = 16.0 Hz), 6.73 (s, 2H, aromatics), 6.31 (d, 1H, CH=CH, J = 16.0 Hz), 4.76 (tt, 1H, CHO, J = 10.8 Hz, J = 4.4 Hz), 3.88 (s, 6H, 2 OCH₃), 3.86 (s, 3H, OCH₃), 3.55 (tt, 1H, CHOH, J = 10.8 Hz, J = 4.0 Hz), 2.60–2.46 (m, 2H, 2NCH), 2.22 (s, 3H, NCH₃), 2.12–1.96 (m, 4H, 2CH₂), 1.89–1.77 (m, 4H, 2CH₂), 1.52–1.22 (m, 8H, 4CH₂) ppm.

cis/cis 18c. ¹H NMR (CDCl₃): δ 7.61 (d, 1H, CH=CH, J = 16.0 Hz), 6.77 (s, 2H, aromatics), 6.34 (d, 1H, CH=CH, J = 16.0 Hz), 5.12–5.07 (m, 1H, CHO), 4.00–3.95 (m, 1H, CHOH), 3.88 (s, 6H, 2 OCH₃), 3.85 (s, 3H, OCH₃), 2.75–2.60 (m, 2H, 2NCH), 2.32 (s, 3H, NCH₃), 2.80–2.00 (m, 2H, CH₂), 1.90–1.69 (m, 8H, 4CH₂), 1.63–1.48 (m, 6H, 3CH₂) ppm.

trans/cis 18d. ¹H NMR (CDCl₃): δ 7.56 (d, 1H, CH=CH, J = 16.0 Hz), 6.73 (s, 2H, aromatics), 6.31 (d, 1H, CH=CH, J = 16.0 Hz), 4.77 (tt, 1H, CHO, J = 10.8 Hz, J = 4.4 Hz), 3.97–3.93 (m, 1H, CHOH), 3.87 (s, 6H, 2OCH₃), 3.86 (s, 3H, OCH₃), 2.69–2.51 (m, 2H, 2NCH), 2.28 (s, 3H, NCH₃), 2.24–2.15 (m, 2H, CH₂), 1.90–1.71 (m, 6H, 3CH₂), 1.60–1.39 (m, 8H, 4CH₂) ppm.

Compound **19a/b** was obtained in the same way from **16a/b**. Its IR and ¹H NMR spectra are consistent with the proposed structures.

3,4,5-Trimethoxybenzoic Acid 4-[tert-Butoxycarbonyl-(4-hydroxycyclohexyl)amino]cyclohexyl Ester (20a/b). To a solution of 260 mg (0.64 mmol) of **14a/b** in 15 mL of THF cooled to 0 °C, 140 mg (0.64 mmol) of di-*tert*-butyldicarbonate, and 0.09 mL of triethylamine were added. The mixture was maintained at room temperature for 10 h and then concentrated in vacuo. The residue was dissolved in CH₂Cl₂, and the organic layer was washed with water. After drying with Na₂SO₄, the solvent was removed under reduced pressure. The crude product was then purified by flash chromatography using CH₂Cl₂/abs EtOH/petroleum ether/NH₄OH 340:65:60:8 as eluting system. Compound **20a/b** (270 mg, 86% yield) was obtained as an oil. IR (neat): ν 3370 (OH), 1706 (CO) cm⁻¹. ¹H NMR (CDCl₃): δ 7.28 (s, 1H, aromatic), 7.29 (s, 1H, aromatic), 5.21 (bs, 0.5H, CHO), 4.99–4.78 (m, 0.5H, CHO), 3.89 (s, 9H, 3OCH₃), 3.61–3.48 (m, 1H, CHOH), 2.28–1.25 (m, 28H, 8CH₂, 3CH₃, 2NCH and OH) ppm.

cis/trans-3,4,5-Trimethoxybenzoic Acid 4-(Methyl[4-[3-(3,4,5-trimethoxyphenyl)acryloyloxy]cyclohexyl]amino)cyclohexyl Ester (3a). Following the procedure described for compound **11**, the acyl chloride obtained from *trans*-3-(3,4,5-trimethoxyphenyl)acryloyl acid (100 mg, 0.43 mmol) was allowed to react with **17a** (120 mg, 0.28 mmol) for 3 h. The crude product was then purified by flash chromatography using CH₂Cl₂/abs. EtOH/ethyl ether/petroleum ether/NH₄OH 360:180:360:900:9.9 as eluting system.

The title compound (43 mg, 30% yield) was obtained as an oil. IR (neat): ν 1713 (CO) cm⁻¹. ¹H NMR (CDCl₃): δ 7.59 (d, J = 15.7 Hz, 1H, CH=CH), 7.34 (s, 2H, aromatics), 6.76 (s, 2H, aromatics), 6.34 (d, J = 15.7 Hz, 1H, CH=CH), 5.21 (bs, 1H, CHO), 4.80 (tt, J = 10.2 Hz, J = 4.4 Hz, 1H, CHO), 3.93 (s, 9H,

3OCH₃), 3.90 (s, 9H, 3OCH₃), 2.70–2.52 (m, 2H, 2NCH), 2.31 (s, 3H, NCH₃), 2.13–1.20 (m, 16H, 8CH₂) ppm. The oily product was transformed into the hydrochloride and recrystallized from absolute ethanol/anhydrous diethylether; mp: 147–150 °C. Anal. (C₃₅H₄₈ClNO₁₀) C, H, N.

Compounds **3b–d**, **4a–d**, **5a–d**, **6a–d**, **7a–c**, **8a–c**, **9a/b**, and **21a/b** were obtained in the same way by reaction of the corresponding alcohol with the suitable acyl chloride. Compounds **3c**, **3d**, **5a–d**, **6a–d**, **7a**, and **8a–c** were transformed into the oxalate, compounds **3b**, **4a–d**, **7b–c**, and **9a/b** were transformed into the hydrochloride and recrystallized from the solvent reported in Table 1. Their chemical and physical characteristics are reported in Table S1, and IR and ¹H NMR spectra are reported in Table S3 (Supporting Information).

3,4,5-Trimethoxybenzoic Acid 4-[4-[3-(3,4,5-Trimethoxyphenyl)acryloyloxy]cyclohexylamino]cyclohexyl Ester (10a/b). To a solution of 110 mg (0.16 mmol) of **21a/b** in 0.32 mL of CH₂Cl₂, 0.32 mL of CF₃COOH were added under vigorous stirring. After 2 h at room temperature, the solution was concentrated in vacuo. The residue was then dissolved in ethyl acetate, and the organic layer was washed with a saturated solution of NaHCO₃. After drying with Na₂SO₄, the solvent was removed under reduced pressure; 90 mg (90% yield) of the pure title compound were obtained. IR (neat): ν 3520 (NH), 1706 (CO) cm⁻¹. ¹H NMR (CDCl₃): δ 7.59 (d, J = 16.0 Hz, 1H, CH=CH), 7.29 (s, 2H, aromatics), 6.76 (s, 2H, aromatics), 6.33 (d, J = 16.0 Hz 1H, CH=CH), 5.17 (bs, 0.5H, CHO), 4.96–4.84 (m, 0.5H, CHO), 4.73–4.81 (m, 1H, CHO), 3.90 (s, 18H, 6OCH₃), 2.71–2.58 (m, 2H, 2NCH), 2.15–1.07 (m, 17H, 8CH₂, NH) ppm.

The oily product was transformed into the hydrochloride, which was recrystallized from absolute ethanol/anhydrous diethylether; mp: 192–194 °C. Anal. (C₃₄H₄₆ClNO₁₀) C, H, N.

Pharmacology. Cell Lines and Cultures. The K562 cell line is a highly undifferentiated erythroleukemia originally derived from a patient with chronic myelogenous leukemia.⁴² The K562 leukemia cells and the P-gp expressing K562/DOX cells were obtained from Prof. J. P. Marie (Hopital Hotel-Dieu, Paris, France). These cells were cultured in RPMI 1640 medium with GlutaMAX-I (GIBCO) medium supplemented with 10% fetal calf serum (FCS) (GIBCO) at 37 °C in a humidified incubator with 5% CO₂. To maintain the resistance, every month, resistant cells were cultured for three days with 400 nM doxorubicin. The cell line was then used, one week later, during three weeks. Cultures initiated at a density of 10⁵ cells/mL grew exponentially to about 10⁶ cells/mL in 3 days. For the spectrofluorometric assays, in order to have cells in the exponential growth phase, culture was initiated at 5 × 10⁵ cells/mL and cells were used 24 h later, when the culture had grown to about 8–10 × 10⁵ cells/mL. Cultured cells were counted with a Coulter counter before use. The viability of the cells, tested by Trypan Blue exclusion, was always greater than 95%.

Modulation of Pirarubicin Uptake. Drugs and Chemicals. Purified pirarubicin was provided by Laboratoire Roger Bellon (France). Concentrations were determined by diluting stock solutions to approximately 10⁻⁵ M and using $\epsilon_{480} = 11500 \text{ M}^{-1} \text{ cm}^{-1}$. Stock solutions were prepared just before use. Buffer solutions were HEPES buffer containing 5 mM HEPES, 132 mM NaCl, 3.5 mM CaCl₂, 5 mM glucose, at pH 7.3.

Cellular Drug Accumulation. The uptake of pirarubicin in cells was followed by monitoring the decrease in the fluorescence signal at 590 nm ($\lambda_{\text{ex}} = 480 \text{ nm}$) according to the previously described method.⁵² Using this method, it is possible to accurately quantify the kinetics of the drug uptake by the cells and the amount of anthracycline intercalated between the base pairs in the nucleus at the steady state, as incubation of the cells with the drug proceeds without compromising cell viability. All experiments were conducted in 1 cm quartz cuvettes containing 2 mL of buffer at 37 °C. We checked that tested compounds did not affect the fluorescence of pirarubicin.

ATPase Activity. Western-Blot Analysis of Intestinal Plasma Membrane Vesicles. Plasma membrane vesicles were prepared from homogenates of rat small intestine mucosa by

differential centrifugation.⁴⁹ Samples of membrane vesicles in loading buffer (1 part of XT reducing agent 20× and 5 parts of XT sample buffer 4×, Bio-Rad), were boiled for 1 min, loaded onto SDS-polyacrylamide electrophoresis gel (Criterion XT, Bio-Rad), and separated by molecular size. Protein concentration was determined by Bradford assay. The gels were then electroblotted onto nitrocellulose membranes (Trans-Blot Transfer-Membrane, Bio-Rad). The surface of the membrane was blocked in TBS solution (Tris-buffered saline and 0.1% Tween 20) containing 5% nonfat milk. Primary antibodies were purchased from Alexis (C219: mouse monoclonal antibody to P-glycoprotein, A23: rabbit polyclonal antibody to Mrp1, M₂III-6: mouse monoclonal antibody to MRP2). Antibodies were diluted in 1% nonfat milk-TBS buffer and incubated overnight at 4 °C. Goat antirabbit IgG-HRP and goat antirabbit IgG-HRP (Santa Cruz Biotechnology) were used as secondary antibodies. Proteins were revealed for colorimetric evaluation (Opti-4CN Substrate Kit, Bio-Rad).

ATPase activity was measured spectrophotometrically at 37 °C using an ATP-regenerating system (pyruvate kinase and phosphoenolpyruvate), coupled to lactate dehydrogenase and NADH, by monitoring NADH absorbance decay with time at 340 nm.^{53,54} Sodium azide, EGTA, and ouabain were added to the reaction medium to inhibit, respectively, H⁺, Ca²⁺, and Na/K-ATPases. NADH absorbance decay with time curve followed a polynomial equation and ATPase activity was calculated by the curve tangent at 1300 s.

Cytotoxicity Assay. Drugs and Chemicals. Doxorubicin hydrochloride (DOX) and verapamil (VRP) drugs were obtained from Sigma; dimethylsulfoxide (DMSO) and 3-(4,5-dimethylthiazolyl-2)-2,5-diphenyltetrazolium bromide (MTT) were purchased from Sigma. MTT stock solution was prepared as follows: 5 mg MTT/mL phosphate saline buffer (PBS) was filtered with 0.45 μm filter units (Nalgene) and stored at 4 °C for a maximum of 1 month. MTT working solution was prepared just before to culture application by diluting MTT stock solution 1:5 in prewarmed culture medium, and 50 μL were added to each culture well, resulting in 0.25 mg MTT/200 μL total medium volume.

Test compounds and DOX stock solutions were prepared in DMSO at 10⁻² M. Verapamil was prepared in water at 10⁻² M. Drugs and test compounds were then diluted with complete medium to obtain the 10× desired final maximum test concentrations. Test compounds were evaluated for cytotoxicity and MDR reversal activity at [I]_{0.5}, 1, and 3 μM, and the corresponding doxorubicin concentrations tested were between 0.001 and 0.1 μM for K562 sensitive cells line and between 0.1 μM and 10 μM for K562/DOX resistant cells.

Verapamil was used as a standard chemomodulator and was evaluated at 1, 1.6 ([I]_{0.5}), and 3 μM. All experiments were carried out in quadruplicate.

MTT Assay. Cells, in exponential growth phase (3–5 × 10⁵ cells/mL), were seeded at 3000 cells/well and either solutions of test compounds or solution of doxorubicin or combination of a solution of doxorubicin and test compounds were added to the wells and the plates were incubated at 37 °C for 72 h in 5% CO₂ incubator. Culture plates were centrifuged at low speed for 5 min, 50 μL of medium was removed from wells and replaced with 50 μL of MTT working solution, and plates were further incubated for 4 h. Following incubation cells and formazan crystals were inspected microscopically. The supernatant was then carefully removed by slow aspiration, and the formazan crystals were dissolved in 100 μL of DMSO; the absorbance of the solution was then read on an automated plate reader at a wavelength of 540 nm.

Acknowledgment. This work was partially supported by the CRF (Ente Cassa di Risparmio di Firenze). We thank Prof. Fulvio Gualtieri for helpful discussion.

Supporting Information Available: Western-blot analysis of intestinal plasma membrane vesicles, chemical and physical characteristics of compounds 3–10, ¹H NMR signals at 400 MHz of compounds 14a–d, 17a–d, 3a–d, 4a–d, IR and ¹H NMR

spectra, and elemental analyses of compounds 3–10. This material is available free of charge via the Internet at <http://pubs.acs.org>.

References

- Mitscher, L. A.; Pillai, S. P.; Gentry, E. J.; Shankel, D. M. Multiple drug resistance. *Med. Res. Rev.* **1999**, *19*, 477–496.
- Volm, M.; Mattern, J. Resistance mechanisms and their regulation in lung cancer. *Crit. Rev. Oncogenesis* **1996**, *7*, 227–244.
- Aszalos, A.; Ross, D. D. Biochemical and clinical aspects of efflux pump related resistance to anti-cancer drugs. *Anticancer Res.* **1998**, *18*, 2937–2944.
- Hrycyna, C. A.; Gottesman, M. M. Multidrug ABC transporters from bacteria to man: an emerging hypothesis for the universality of molecular mechanism and functions. *Drug Resist. Updates* **1998**, *1*, 81–83.
- Kuhnke, D.; Jedlitschky, G.; Grube, M.; Krohn, M.; Jucker, M.; Mosyagin, I.; Cascorbi, I.; Walker, L. C.; Kroemer, H. K.; Warzog, R. W.; Vogelgesang, S. MDR1-P-Glycoprotein (ABCB1) mediates transport of Alzheimer's amyloid-beta peptides implications for the mechanism of Abeta clearance at the blood-brain barrier. *Brain Pathol.* **2007**, *17*, 347–353.
- Johnstone, R. W.; Rueffli, A. A.; Smyth, M. J. Multiple physiological functions for multidrug transporter P-glycoprotein. *Trends Biochem. Sci.* **2000**, *25*, 1–6.
- Rosenberg, M. F.; Kamis, A. B.; Callaghan, R.; Higgins, C. F.; Ford, R. C. Three dimensional structures of the mammalian multidrug-resistant P-glycoprotein demonstrate major conformational changes in the transmembrane domain upon nucleotide binding. *J. Biol. Chem.* **2003**, *278*, 8294–8299.
- Rosenberg, M. F.; Callaghan, R.; Modok, S.; Higgins, C. F.; Ford, R. C. Three-dimensional structure of P-glycoprotein. *J. Biol. Chem.* **2005**, *280*, 2857–2862.
- Ward, A.; Reyes, C. L.; Yu, J.; Roth, C. B.; Chang, G. Flexibility in the ABC transporter MsbA: alternating access with a twist. *Proc. Natl. Acad. Sci. U.S.A.* **2007**, *104*, 19005–19010.
- Dawson, R. J.; Locher, K. P. Structure of a bacterial multidrug ABC transporter. *Nature* **2006**, *443*, 180–185.
- Dawson, R. J.; Locher, K. P. Structure of the multidrug ABC transporter Sav1866 from *Staphylococcus aureus* in complex with AMP-PNP. *FEBS Lett.* **2007**, *581*, 935–938.
- Zolnercik, J. K.; Wooding, C.; Linton, K. J. Evidence for a Sav1866-like architecture for the human multidrug transporter P-glycoprotein. *FASEB J.* **2007**, *21*, 3937–3948.
- O'Mara, M. L.; Tieleman, D. P. P-glycoprotein models of the apo and ATP-bound states based on homology with Sav1866 and MalK. *FEBS Lett.* **2007**, *581*, 4217–4222.
- Globisch, C.; Pajeva, I. K.; Wiese, M. Identification of putative binding sites of P-glycoprotein based on its homology model. *ChemMedChem* **2008**, *3*, 280–295.
- Gottesman, M. M.; Fojo, T.; Bates, S. E. Multidrug resistance in cancer: role of ATP-dependent transporters. *Nat. Rev. Cancer* **2002**, *2*, 48–58.
- Murray, D. S.; Schumacher, M. A.; Brennan, R. G. Crystal structure of QacR–diamidine complexes reveal additional multidrug-binding modes and a novel mechanism of drug charge neutralization. *J. Biol. Chem.* **2004**, *279*, 14365–14371.
- Schumacher, M. A.; Miller, M. C.; Brennan, R. G. Structural mechanism of the simultaneous binding of two drugs to a multidrug binding protein. *EMBO J.* **2004**, *23*, 2923–2930.
- Teodori, E.; Dei, S.; Martelli, C.; Scapecchi, S.; Gualtieri, F. The functions and structure of ABC transporters: implications for the design of new inhibitors of Pgp and MRP1 to control multidrug resistance (MDR). *Curr. Drug Targets* **2006**, *7*, 893–909.
- Nobili, S.; Landini, I.; Gigliani, B.; Mini, E. Pharmacological strategies for overcoming multidrug resistance. *Curr. Drug Targets* **2006**, *7*, 861–879.
- Avendano, C.; Menendez, J. C. Inhibitors of multidrug resistance to antitumor agents (MDR). *Curr. Med. Chem.* **2002**, *9*, 159–193.
- Fusi, F.; Saponara, S.; Valoti, M.; Dragoni, S.; D'Elia, P.; Sgaragli, T.; Alderighi, D.; Kawase, M.; Shah, A.; Motohashi, N.; Sgaragli, G. Cancer cell permeability-glycoprotein as a target of MDR reverters: possible role of novel dihydropyridine derivatives. *Curr. Drug Targets* **2006**, *8*, 949–959.
- Robert, J.; Jarry, C. Multidrug resistance reversal agents. *J. Med. Chem.* **2003**, *46*, 4805–4817.
- Sorbera, L. A.; Castaner, J.; Silvestre, J. S.; Bayés, M. Zosuquidar trihydrochloride. *Drugs Future* **2003**, *28*, 125–136.
- Szakács, G.; Paterson, J. K.; Ludwig, J. A.; Booth-Genthe, C.; Gottesman, M. M. Targeting multidrug resistance in cancer. *Nat. Rev. Drug. Discovery* **2006**, *5*, 219–34.
- Tan, B.; Piwnicka-Worms, D.; Ratner, L. Multidrug resistance transporters and modulation. *Curr. Opin. Oncol.* **2000**, *12*, 450–458.

- (26) Teodori, E.; Dei, S.; Garnier-Suillerot, A.; Gualtieri, F.; Manetti, D.; Martelli, C.; Romanelli, M. N.; Scapecchi, S.; Paiwan, S.; Salerno, M. Exploratory chemistry toward the identification of a new class of MDR reverters inspired by pervilleine and verapamil models. *J. Med. Chem.* **2005**, *48*, 7426–7436.
- (27) Wenlock, M. C.; Austin, R. P.; Barton, P.; Davis, A. M.; Leeson, P. D. A comparison of physicochemical properties profiles of development and marketed oral drugs. *J. Med. Chem.* **2003**, *46*, 1250–1256.
- (28) Veber, D. F.; Johnson, S. R.; Cheng, H.-Y.; Smith, B. R.; Ward, K. W.; Kopple, K. D. Molecular properties that influence the oral bioavailability of drug candidates. *J. Med. Chem.* **2002**, *45*, 2615–2623.
- (29) Gualtieri, F.; Romanelli, M. N.; Teodori, E. The frozen analog approach in medicinal chemistry. *Progress in Medicinal Chemistry*; Harwood Academic Publishers: Amsterdam, 1996, 271–317.
- (30) Teodori, E.; Martelli, C.; Salerno, M.; Darghal, N.; Dei, S.; Garnier-Suillerot, A.; Gualtieri, F.; Manetti, D.; Scapecchi, S.; Romanelli, M. N. Isomeric N,N-bis(cyclohexanol)amine aryl esters: the discovery of a new class of highly potent Pgp-dependent multidrug resistance (MDR) inhibitors. *J. Med. Chem.* **2007**, *50*, 599–602.
- (31) Litman, T.; Druley, T. E.; Stein, W. D.; Bates, S. E. From MDR to MXR: new understanding of multidrug resistance systems, their properties and clinical significance. *Cell. Mol. Life Sci.* **2001**, *58*, 931–959.
- (32) Wiese, M.; Pajeva, K. Structure activity relationships of multidrug resistance reversers. *Curr. Med. Chem.* **2001**, *8*, 685–713.
- (33) Polli, J. W.; Wring, S. A.; Humphreys, J. E.; Huang, L.; Morgan, J. B.; Webster, L. O.; Serabjit-Singh, C. O. Rational use of in vitro P-glycoprotein assays in drug discovery. *J. Pharmacol. Exp. Ther.* **2001**, *299*, 620–628.
- (34) Tomioka, H.; Oshima, K.; Nozaki, H. Cerium catalyzed selective oxidation of secondary alcohols in the presence of primary ones. *Tetrahedron Lett.* **1982**, *23*, 539–542.
- (35) Franciskovich, J. B.; Herron, D. K.; Linebarger, J. H.; A.L., M.; Masters, J. J.; Mendel, D.; Merritt, L.; Ratz, A. M.; Smith, G. F.; Weigel, L. O.; Wiley, M. R.; Yee, Y. K. Preparation of N-(2-pyridyl)-3-(benzoylamino)pyridine-2-carboxamide derivatives as antithrombotics Patent WO 2004108677, 2004.
- (36) Mattson, R. J.; Pham, K. M.; Leuck, D. J.; Cowen, K. A. An improved Method for Reductive Alkylation of Amines Using Titanium(IV) Isopropoxide and Sodium Cyanoborohydride. *J. Org. Chem.* **1990**, *55*, 2552–2554.
- (37) de Oliveira, P. R.; Wiectzycosky, F.; Basso, E. A.; Goncalves, R. A. C.; Pontes, R. M. Structural characterization of two novel potential anticholinesterasic agents. *J. Mol. Struct.* **2003**, *657*, 191–198.
- (38) Dei, S.; Budriesi, R.; Paiwan, S.; Ferraroni, M.; Chiarini, A.; Garnier-Suillerot, A.; Manetti, D.; Martelli, C.; Scapecchi, S.; Teodori, E. Diphenylcyclohexylamine derivatives as new potent multidrug resistant (MDR) modulators. *Bioorg. Med. Chem.* **2005**, *13*, 985–998.
- (39) Zhang, S.; Reith, M. E. A.; Dutta, A. K. Design, synthesis, and activity of novel *cis*- and *trans*-3,6-disubstituted pyran biomimetics of 3,6-disubstituted piperidine as potential ligands for the dopamine transporter. *Bioorg. Med. Chem. Lett.* **2003**, *13*, 1591–1595.
- (40) Vergote, J.; Moretti, J. L.; De Vries, E. G. E.; Garnier-Suillerot, A. Comparison of the kinetics of active efflux of ^{99m}Tc-MIBI in cells with P-glycoprotein-mediated and multidrug-resistance protein-associated multidrug-resistance phenotype. *Eur. J. Biochem.* **1998**, *252*, 140–146.
- (41) Reungpatthanaphong, P.; Marbeuf-Gueye, C.; Le Moyec, L.; Salerno, M.; Garnier-Suillerot, A. Decrease of P-glycoprotein activity in K562/ADR cells by MβCD and filipin and lack of effect induced by cholesterol oxidase indicate that this transporter is not located in rafts. *J. Bioenerg. Biomembr.* **2004**, *36*, 533–543.
- (42) Lozio, C. B.; Lozzio, B. B. Human chronic myelogenous leukemia cell line positive philadelphia chromosome. *Blood* **1975**, *45*, 321–334.
- (43) Tsuroo, T.; Ida, H.; Kawataba, H.; Oh-Hara, T.; Hamada, H.; Utakoji, T. Characteristics of resistance to adriamycin in human myelogenous leukemia K562 resistant to adriamycin and in isolated clones. *Jpn. J. Cancer Res* **1986**, *77*, 682–687.
- (44) Dei, S.; Teodori, E.; Garnier-Suillerot, A.; Gualtieri, F.; Scapecchi, S.; Budriesi, R.; Chiarini, A. Structure–activity relationships and optimisation of the selective MDR modulator 2-(3,4-dimethoxyphenyl)-5-(9-fluorenylamino)-2-(methyl ethyl) pentanenitrile (SC11) and its N-methyl derivative (SC17). *Bioorg. Med. Chem.* **2001**, *9*, 2673–2682.
- (45) Pereira, E.; Garnier-Suillerot, A. Correlation between the short-term measurements of drug accumulation in living cells and the long-term growth inhibition. *Biochem. Pharmacol.* **1994**, *47*, 1851–1857.
- (46) Teodori, E.; Dei, S.; Quidu, P.; Budriesi, R.; Chiarini, A.; Garnier-Suillerot, A.; Gualtieri, F.; Manetti, D.; Romanelli, M. N.; Scapecchi, S. Design, synthesis, and in vitro activity of catamphiphilic reverters of multidrug resistance: discovery of a selective, highly efficacious chemosensitizer with potency in the nanomolar range. *J. Med. Chem.* **1999**, *42*, 1687–1697.
- (47) Higgins, C. F.; Linton, K. J. The ATP switch model for ABC transporters. *Nat. Struct. Mol. Biol.* **2004**, *11*, 918–926.
- (48) Sauna, Z. E.; Kim, I. W.; Nandigama, K.; Kopp, S.; Chiba, P.; Ambudkar, S. V. Catalytic cycle of ATP hydrolysis by P-glycoprotein: evidence for formation of E.S reaction intermediate with ATP-gamma-S, a nonhydrolyzable analog of ATP. *Biochemistry* **2007**, *46*, 13787–13799.
- (49) Shirazi, S. P.; Beechey, R. B.; Butterworth, P. J. The use of potent inhibitors of alkaline phosphatase to investigate the role of the enzyme in intestinal transport of inorganic phosphate. *Biochem. J.* **1981**, *194*, 803–9.
- (50) Alley, M. C.; Scudiero, D. A.; Monks, A.; Hursey, M. L.; Czerwinski, M. J.; Fine, D. L.; Abbott, B. J.; Mayo, J. G.; Shoemaker, R. H.; Boyd, M. R. Feasibility of drug screening with panels of human tumour cell lines using a microculture tetrazolium assay. *Cancer Res.* **1988**, *48*, 589–601.
- (51) Sarkadi, B.; Homolya, L.; Szakács, G.; Váradi, A. Human multidrug resistance ABCB and ABCG transporters: participation in a chemoinmunity defense system. *Physiol. Rev.* **2006**, *86*, 1179–1236.
- (52) Mankehetkorn, S.; Garnier-Suillerot, A. The ability of verapamil to restore intracellular accumulation of anthracyclines in multidrug resistant cells depends on the kinetics of their uptake. *Eur. J. Pharmacol.* **1998**, *343*, 313–321.
- (53) Schar Schmidt, B. F.; Keeffe, E. B.; Blankenship, N. M.; Ockner, R. K. Validation of a recording spectrophotometric method for measurement of membrane-associated Mg- and NaK-ATPase activity. *J. Lab. Clin. Med.* **1979**, *93*, 790–9.
- (54) Garrigues, A.; Nugier, J.; Orlowski, S.; Ezan, E. A high-throughput screening microplate test for the interaction of drugs with P-glycoprotein. *Anal. Biochem.* **2002**, *305*, 106–114.